Eur Biophys J (2008) 37:913–925
DOI 10.1007/s00249-008-0309-9

ORIGINAL PAPER

Excursion of a single polypeptide into a protein pore: simple physics, but complicated biology

Mohammad M. Mohammad · Liviu Movileanu

Received: 30 September 2007 / Revised: 4 January 2008 / Accepted: 10 March 2008 / Published online: 27 March 2008

Abstract Despite its fundamental and critical importance in molecular biology and practical medical biotechnology, how a polypeptide interacts with a transmembrane protein pore is not yet comprehensively understood. Here, we employed single-channel electrical recordings to reveal the interactions of short polypeptides and small folded proteins with a robust β-barrel protein pore. The short polypeptides were $\sim$25 residues in length, resembling positively charged targeting presequences involved in protein import. The proteins were consisted of positively charged pre-cytochrome b_2 fragments (pb_2) fused to the small ribonuclease barnase ($\sim$110 residues, Ba). Single-molecule experiments exploring the interaction of a folded pb_2-Ba protein with a single β-barrel pore, which contained negatively charged electrostatic traps, revealed the complexity of a network of intermolecular forces, including driving and electrostatic ones. In addition, the interaction was dependent on other factors, such as the hydrophobic content of the interacting polypeptide, the location of the electrostatic trap, the length of the pb_2 presequence and temperature. This single-molecule approach together with protein design of either the interacting polypeptide or the pore lumen opens new opportunities for the exploration of the polypeptide–pore interaction at high temporal resolution. Such future studies are also expected to unravel the advantages and limitations of the nanopore technique for the detection and exploration of individual polypeptides.

Keywords Protein translocation · Electrophysiology · Electrostatic interaction · Protein design · Presequence · Single-molecule biophysics

M. M. Mohammad · L. Movileanu (✉)
Department of Physics, Syracuse University,
201 Physics Building, Syracuse, NY 13244-1130, USA
e-mail: lmovilea@physics.syr.edu

L. Movileanu
Structural Biology, Biochemistry, and Biophysics Program,
Syracuse University, 111 College Place, Syracuse,
NY 13244-4100, USA

Introduction

A transmembrane β-barrel protein represents a general scaffold used by protein-conducting protein pores. For example, the translocation of proteins into mitochondria, chloroplasts and Gram-negative bacteria occurs through a transmembrane β-barrel pore located in the outer membrane (Gabriel et al. 2001; Matouschek and Glick 2001). A β-barrel pore may also serve as a protein tunnel for enzymes to enter the cytosol (Krantz et al. 2005; Halverson et al. 2005; Karginov et al. 2005). The 263-residue N-terminal fragment of LF (LF_N) is translocated even in the absence of cellular proteins or ATP-driven cellular factors across the protective antigen channel (PA_{63}) of anthrax toxin (Krantz et al. 2005, 2006). This translocation machinery is apparently similar to that in C*lostridial botulinum* neurotoxins (BoNTs), which act as a transmembrane chaperone (Koriazova and Montal 2003; Fischer and Montal 2007). Previous studies using reconstituted lipid membranes to address many of the fundamental questions pertinent to polypeptide translocation have been hampered by a number of technical challenges, including the considerable complexity in the translocation machineries employing several proteins (Wickner and Schekman 2005), a lack of sufficient structural information (Wickner and Schekman 2005), and the complications caused by intrinsic gating current sub-states of most protein

translocases in mitochondria (Muro et al. 2003; Becker et al. 2005), chloroplasts (Hinnah et al. 2002), and Gram-negative bacteria (Zakharov et al. 2004).

In this work, we propose that *Staphylococcal aureus* α-hemolysin (αHL) is a suitable model for a β-barrel pore for studying polypeptide translocation. αHL is a heptameric mushroom-shaped protein of known high-resolution crystal structure (Song et al. 1996) (Fig. 1). αHL forms well-defined homoheptameric pores in lipid bilayers (Song et al. 1996; Krasilnikov et al. 2000). In the transmembrane domain, the αHL channel forms a β-barrel region with an average diameter of ~20 Å (Song et al. 1996). This is similar to the effective internal diameter of the protein import channel in the outer membrane of mitochondria (~20 Å) (Schwartz and Matouschek 1999; Muro et al. 2003). Explorations employing poly(ethylene glycol)s (PEGs) for determining the internal pore geometry of the Toc75 translocase from the outer membrane of chloroplasts indicated a diameter of ~22 Å (Hinnah et al. 2002).

There are several strong motivations behind using αHL protein for studies on polypeptide translocation. The αHL pore is always in a single orientation with respect to the bilayer, and exhibits a well-defined high single-channel conductance (e.g., 950 pS in 1 M KCl, pH 7.5, +100 mV) (Movileanu et al. 2003, 2005). The αHL pore is open for long periods of time even in extreme conditions of pH (i.e., from 4 to 11) (Misakian and Kasianowicz 2003), transmembrane potential (i.e., up to 160 mV) (Menestrina 1986), temperature (i.e., 0–95 °C) (Kang et al. 2005), salt concentration (i.e., 0.1–4.0 M KCl) (Krasilnikov et al. 2006), osmotic pressure (i.e., a few tens of % (w/v) (polyethylene glycol)s) (Krasilnikov and Bezrukov 2004) and chemical denaturants (i.e., guanidinium hydrochloride) (Oukhaled et al. 2007). Therefore, the αHL protein may serve as a blank state for the polypeptide translocation through a β-barrel transmembrane pore.

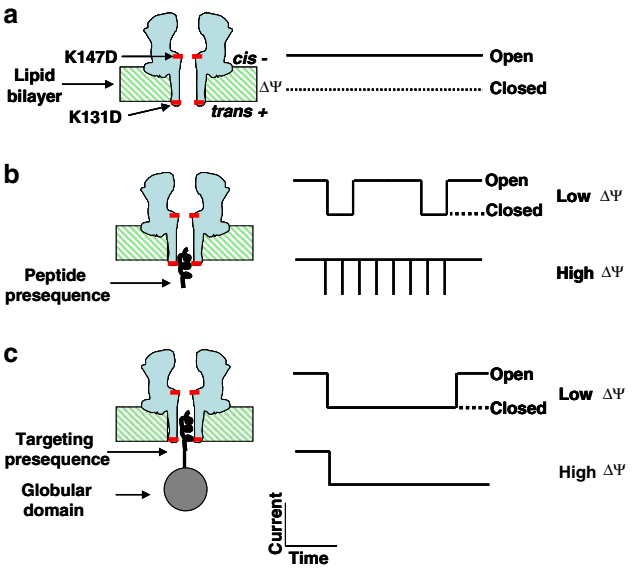

Fig. 1 Interaction of a single polypeptide with a robust β-barrel protein pore containing electrostatic traps. **a** Sectional view of the αHL pore with engineered electrostatic traps shown by *arrows*. K131D and K147D mutations introduced an acidic ring of aspartic acids on either the *trans* or *cis* end of the β barrel or both, **b** a short, positively charged polypeptide interacts with the negatively charged traps located on the pore walls. Partitioning of the short polypeptide into the pore lumen is accompanied by transient current blockades, the nature which is dependent on the features of the polypeptide and engineered αHL pore, **c** a folded pb_2-Ba protein partitions into the αHL protein pore from the *trans* side of the bilayer. Partitioning of a single pb_2-Ba protein into the pore lumen is observed by long-lived current blockades in the single-channel electrical traces

In this work, the interacting polypeptides were targeted to the pore lumen through attractive electrostatic interactions between their positively charged residues and the negatively charged traps of aspartic acid residues engineered within the β-barrel part of the pore (Fig. 1a). The translocating polypeptides were either short model and presequence polypeptides (Fig. 1b) or folded pb_2-Ba proteins (Fig. 1c) consisted of the positively charged N-terminal region of pre-cytochrome b_2 (pb_2) fused to the N terminus of the small ribonuclease barnase (Ba) (Huang et al. 2002). Mitochondrial presequences have negligible secondary structure in solution (Roise et al. 1988), and they are exposed to aqueous phase when fused to the folded Ba domain (Matouschek et al. 1997). The $pb_2(35)$, $pb_2(65)$ and $pb_2(95)$ presequences contain the first 35, 65 and 95 residues, respectively, of the pre-cytochrome b_2. They would have the length of ~120, ~224 and ~329 Å, respectively, in a fully extended conformation, which is much longer than the length of the β-barrel part of the pore (~50 Å). The folded Ba domain has an ellipsoidal shape with the long and wide sides of ~43 and ~35 Å, respectively (Mauguen et al. 1982). These dimensions are much greater than the narrowest inner diameter of the αHL protein pore (~15 Å) (Song et al. 1996).

Here, the polypeptide–pore interaction was explored by single-channel electrical recordings of the wild type and engineered αHL pores reconstituted on a planar lipid bilayer, probing the frequency and duration of transient polypeptide-induced current blockades (Sackmann and Neher 1995; Movileanu et al. 2005). This experimental design allowed the direct determination of the rate constants of association and dissociation of the polypeptide-pore interaction. The major fundamental question in this work was, "how sensitive are the single-molecule nanopore recordings with the changes in biophysical features of the pore lumen or the interacting polypeptide?" This question was driven by the idea that these concurrent measurements of the rate constants of association and dissociation might allow us a better understanding of the

biophysical mechanisms that govern polypeptide transport across a protein channel (Simon et al. 1992).

Therefore, we examined the changes of the single-channel kinetics with systematic modifications of an array of biophysical factors, including the hydrophobic content of the polypeptides, their residual helical structure in solution, the position of the electrostatic trap within the pore lumen, the length of the positively charged pb_2 presequence of the small pb_2-Ba proteins, and the temperature. This study illuminated critically important kinetic information about the polypeptide–pore interaction, which is instrumental for understanding the molecular mechanisms involved in the polypeptide-pore interaction. The second question was, "could we design a simple model of the free-energy landscape accounting for the underlying kinetics between the short polypeptides and the electrostatic trap-containing αHL pore?" In the third part of the paper, we present single-channel recordings employing small folded polypeptides, increasing the complexity of the polypeptide-pore interaction.

Materials and methods

Polypeptides: design, synthesis and purification

Syn B2 = MLSRQQSQRQSRQQSQRQSRYLL (M_W = 2.9 kDa), Cox IV = MLSLRQSIRFFKPATRTLCSSRY (2.8 kDa) and AK = $(AAKAA)_5Y\text{-}NH_2$ (2.2 kDa), and AK_{DL} = Ac-$(A_DA_LKA_DA_L)_5Y\text{-}NH_2$ (2.2 kDa). All polypeptide samples had an HPLC purity of at least 95% (GenScript, Scotch Plains, NJ). The polypeptides were synthesized by an automatic solid-phase method using an active ester coupling procedure with Fmoc-amino acids (Goodrich et al. 2007), purified by reversed-phase HPLC, and confirmed by MALDI-TOF mass spectrometry and analytical HPLC (GenScript, Scotch Plains, NJ).

Expression and purification of the pb_2-Ba proteins

The substrate proteins consisted of presequences containing the first 35, 65 or 95 amino acids of yeast precytochrome b_2 (pb_2) fused to the N terminus of the small ribonuclease barnase (Ba) (Guiard 1985; Paddon and Hartley 1987). We used the following nomenclature: pb_2(35)-Ba, pb_2(65)-Ba and pb_2(95)-Ba, respectively. Cysteine, at position 30 in the pb_2 presequence, was mutated to valine (C14V) to prevent disulfide bonds between the fused presequences. Histidine 102 in the Ba domain was also mutated to alanine (H102A) for the inactivation of protein during its expression in *E. coli*. The genes for the three different precursors were inserted under the *lac* promoter into the pQE60 plasmids. *E. coli* M15 cells were transformed with the plasmids encoding the pb_2-Ba proteins, and induced by IPTG. After 20 min, the cells were pulsed with 0.4 mg/ml leucine. Cells were harvested and re-suspended in the breaking buffer (50 mM NaOAc/HOAc pH 5, 1 mM PMSF, 2 mM EDTA, 5 mM benzamidine), and then sonicated on ice and spun down at 4°C. Pellets were re-suspended in the washing buffer (50 mM NaOAc/HOAc, pH 5, 1% (w/v) Triton, 200 mM NaCl, 1 mM PMSF, 2 mM EDTA, 5 mM benzamidine). This step was repeated three times and the final pellets were re-suspended in the extraction buffer (50 mM NaOAc/HOAc, 6 M guanidine hydrochloride, 0.1% (w/v) Triton, 0.5 mM PMSF, 2 mM EDTA, 5 mM DTT, 1 μg/ml leupeptin, 1 μg/ml antipain, pH 5). Pellets were homogenized and the resultant solutions were spun down at 130,000 g for one hour, and at 4°C. The supernatants were dialyzed against the dialysis buffer (50 mM NaOAc/HOAc, 1.5 M guanidine hydrochloride, 0.5 mM PMSF, 2 mM EDTA, pH 5) for 3 h at 4°C. The supernatants were diluted into 50 ml dilution buffer (50 mM NaOAc/HOAc, 2 mM EDTA, 5 mM DTT, pH 5). The proteins were concentrated by Amicon 50 ml stirred cell at 4°C (~8–10 mg per liter of the cell culture).

Expression and purification of the αHL pores

The $K131D_7$, $K147D_7$ and $K131D_7/K147D_7$ mutants were made from the *αHL* gene in the plasmid that was synthetically constructed to produce unique restriction sites (αHL-RL3). Briefly, the K131D and K147D mutants were constructed by PCR-based recombination as previously described (Movileanu et al. 2001; Wolfe et al. 2007). The K131D/K147D mutant was constructed by cassette mutagenesis (Movileanu et al. 2001; Wolfe et al. 2007). The αHL proteins were synthesized in vitro by coupled transcription and translation (IVTT) in the presence of rabbit erythrocyte membranes as previously described (Cheley et al. 1999; Movileanu et al. 2001). The [^{35}S]methionine-labeled polypeptides were purified on an 8% SDS-polyacrylamide gel. The dried gel was autoradiographed and the bands corresponding to each αHL protein pore were excised and rehydrated in 500 μl of MilliQ water. Gel fragments were removed with a spin filter and the resulting filtrate was stored frozen in 50-μl aliquots at −80°C. The αHL model (7ahl.pdb) was generated with the PyMol software (Delano 2007).

Electrical recordings in planar bilayers

Electrical recordings were carried out with planar bilayer lipid membranes (BLMs) (Movileanu et al. 2000; Movileanu and Bayley 2001). The *cis* and *trans* chambers of the apparatus were separated by a 25-μm-thick Teflon

septum (Goodfellow Corporation, Malvern, PA). A 1,2 diphytanoyl-*sn*-glycerophosphatidylcholine (Avanti Polar Lipids, Alabaster, AL) bilayer was formed across a 60-μm-wide aperture in the septum. The electrolyte in both chambers was 1 M KCl, 10 mM potassium phosphate, pH 7.4. The αHL pores were introduced by adding gel-purified heptamers (0.5–2.0 μl) to the *cis* chamber to give a final protein concentration of 0.05–0.3 ng/ml. Single-channel currents were recorded by using a patch clamp amplifier (Axopatch 200B, Axon Instruments, Foster City, CA) connected to Ag/AgCl electrodes through agar bridges. The *cis* chamber was grounded and a positive current (upward deflection) represents positive charge moving from the *trans* to *cis* side. A Pentium PC (Dell, Austin, TX) was equipped with a DigiData 1322A A/D converter (Axon) for data acquisition. The signal was low-pass filtered with an 8-pole Bessel filter (Frequency Devices, Ottawa, IL) at a frequency of 10 kHz and sampled at 100 kHz. For data acquisition and analysis, we used the pClamp9.2 software package (Axon). The temperature-control experiments were carried out by using a Dagan HCC-100A controller (Dagan Corporation, Minneapolis, MN), which was adapted to planar bilayer recordings (Jung et al. 2006). The HCC-100A heated and cooled an aluminum thermal stage through Peltier elements. Temperature was simultaneously monitored in the aluminum stage and in the bilayer chamber with thermocouple probes (Jung et al. 2006).

Determination of the kinetic rate constants

The polypeptide-pore interaction was analyzed by the rate constant of association (k_{on}) and dissociation (k_{off}) (Movileanu et al. 2000; Howorka et al. 2001). The rate constants of association k_{on} were derived from the slopes of plots of $1/\tau_{on}$ versus [polypept], where polypept is the polypeptide concentration in the aqueous phase (see below). The rate constants for dissociation (k_{off}) were determined by averaging the $1/\tau_{off}$. Therefore, one can intuitively get some information from the single-channel electrical trace: the frequency of events is proportional with the rate constant of association k_{on}, whereas the mean of the reciprocal of the event duration is the rate constant of dissociation k_{off}.

The dwell time histograms (τ_{off}) exhibited a well-defined double-exponential distribution, with short-lived ($\tau_{off\text{-}1}$) and long-lived ($\tau_{off\text{-}2}$) events, as judged by a log likelihood ratio (LLR) test (McManus and Magleby 1988; Movileanu et al. 2005). The substrate escapes the αHL protein pore through either the *trans* or *cis* opening, so the total rate constant of dissociation has the relationship $k_{off\text{-}2} = k^{cis}_{off\text{-}2} + k^{trans}_{off\text{-}2}$, where $k_{off\text{-}2} = 1/\tau_{off\text{-}2}$, and $\tau_{off\text{-}2}$ is the mean dwell time of the long-lived events (Movileanu et al. 2005). The rate constants of association $k_{on\text{-}1}$ and $k_{on\text{-}2}$ were calculated as $f_1 k_{on}$ and $f_2 k_{on}$, respectively (Movileanu et al. 2003). Here, f_1 and f_2 are the probabilities of the short-lived events "1" and long-lived events "2", respectively. They were determined from the dwell time histograms (Movileanu et al. 2003). The voltage-dependence of the rate constant of dissociation $k_{off\text{-}2}$ underwent a crossover behavior that reflected the *cis* and *trans* components of the polypeptide escape, indicating the transition from *trans*-favored dissociation to *cis*-favored dissociation (see below) (Movileanu et al. 2005).

Results and discussion

Interaction of a short polypeptide with a transmembrane protein pore

First, we explored the interaction of short polypeptides with a single transmembrane protein pore, which contained an electrostatic trap engineered at the strategic position of the lumen. The electrostatic trap was located on the *trans* entrance of the pore lumen ($K131D_7$), on the *cis* end of the β barrel ($K147D_7$) or both (Fig. 1a). In both single-site mutants, a lysine was replaced by an aspartic acid. Due to the stoichiometry of the αHL protein pore, each single-site mutation in the monomer resulted in seven-residue replacements in the heptameric pore, creating an acidic iris composed of aspartic acid side chains. The additive effect of both engineered traps was further revealed by the double-trap-containing αHL protein pore ($K131D_7/K147D_7$), introducing an alteration of -28 net charge in the pore lumen compared with the wild-type αHL (WT-αHL) protein pore.

We selected four polypeptides ("Materials and methods"): an alanine-based AK polypeptide with the repeat unit AAKAA (Movileanu et al. 2005), an AK_{DL} polypeptide, a mitochondrial presequence Cox IV and a synthetic hydrophilic presequence Syn B2 (Hinnah et al. 2002; Muro et al. 2003). AK_{DL} is an alanine-based polypeptide that shares sequence homology with the AK polypeptide, but with alternating chirality forms (dextro and levo). AK is the only polypeptide with a high α-helical structure in aqueous phase (~56%) (Movileanu et al. 2005). The alteration of the chirality of the amino acids alters completely the α-helical structure of the AK polypeptide. Several studies have demonstrated that D-amino acids alternating with L-amino acids destabilize the α-helical regions in both proteins and peptides (Krause et al. 2000; Mitchell and Smith 2003; Chen et al. 2003). By using temperature-dependent circular dichroism measurements, we found that the AK_{DL} polypeptide is completely unfolded (data not shown), which is in accord with these prior studies. These polypeptides were similar in length (~25

residues) and charge (~+5) at pH 7.4, but they differed greatly in their hydropathy index: 15.2 (AK and AK_{DL}), -5.2 (Cox IV) and -44.4 (Syn B2), respectively (Kyte and Doolittle 1982).

When inserted into a planar lipid bilayer, the wild type and engineered αHL channels remained open for long periods (data not shown). At low micromolar concentrations of polypetides, transient current blockades were observed, the nature of which was dependent on both the features of the electrostatic trap-containing αHL pore and the polypeptides (Fig. 2). Our single-channel experiments (Sackmann and Neher 1995) were performed with the polypeptide/protein sample added only to the *trans* side, since the *cis* side of the αHL protein protrudes far in the aqueous phase, ~50 Å away from the bilayer surface (Fig. 1a), leading to complications in the interpretation of the single-channel data. It is likely that these complications are caused by the complexity of the free-energy landscape when the polypeptides are added to the *cis* side of the lipid bilayer. In contrast, the transmembrane domain of the pore forming a roughly cylindrical β-barrel tunnel is near aqueous phase, which simplifies the free-energy landscape for partitioning of bulky polypeptides into the pore lumen.

Figure 2 illustrates the effect of the Cox IV polypeptide on the single-channel electrical signature of the WT-αHL and electrostatic trap-containing αHL protein pores. In general, the dwell time histograms showed a two-exponential distribution of the transient polypeptide-produced current blockades in single-channel recordings with the WT-αHL and engineered αHL protein pores. The two-exponential distribution was judged by a LLR test (Movileanu et al. 2003, 2005), providing the mean dwell times of the short-lived ($\tau_{off\text{-}1}$) and long-lived ($\tau_{off\text{-}2}$) events.

At low micromolar concentrations of short polypeptides, we found that the dwell time of the long-lived events $\tau_{off\text{-}2}$ (the mean dwell time of the long-lived events from the

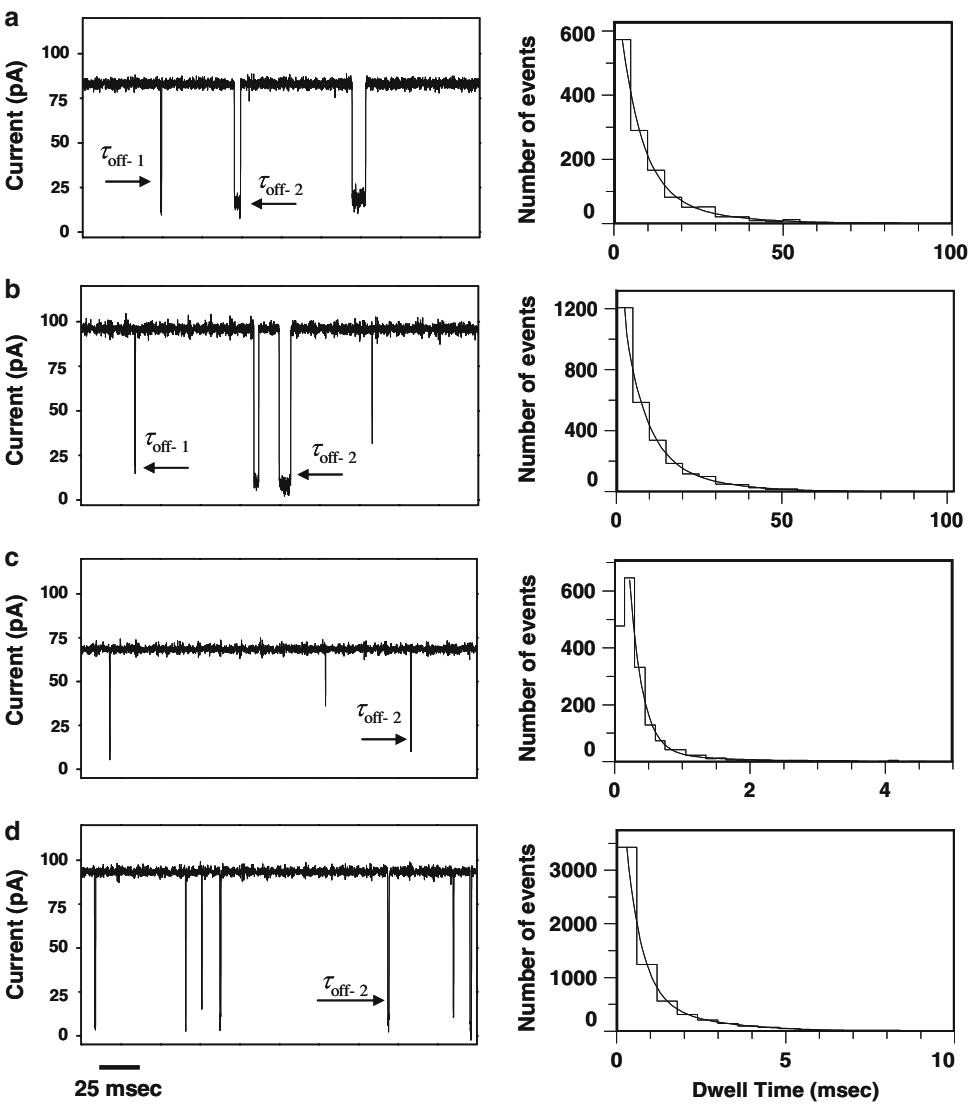

Fig. 2 Representative single-channel electrical recordings with the wild-type and engineered αHL protein pores in the presence of 34 μM of the Cox IV polypeptide added to the *trans* side of the lipid bilayer: **a** WT-αHL, **b** $K131D_7$, **c** $K147D_7$, **d** $K131D_7/K147D_7$. The frequency and duration of the polypeptide-induced current blockades were dependent on the position of the electrostatic trap. All traces were recorded in symmetrical buffer conditions (1 M KCl, 10 mM potassium phosphate, pH 7.4), and at a transmembrane potential of +80 mV. The *smooth curves* from the right-handed dwell time histograms were either double-exponential (for **a** and **b**) or single-exponential (for **c** and **d**) fits. The single-channel electrical traces were low-pass Bessel filtered at 2 kHz

histogram of the occupied states) is independent of the polypeptide concentration (Fig. 3a), whereas the reciprocal of the mean inter-event interval τ_{on} is linearly dependent on the polypeptide concentration (Fig. 3b). Thus, a simple bimolecular interaction between the polypeptide and the pore can be assumed. On the other hand, the short-lived events ($\tau_{off\text{-}1}$) were not voltage dependent (Fig. 3c), and were interpreted as simple collisions of the polypeptides with the opening of the pore. Therefore, the rate constant of dissociation $k_{off\text{-}1}$ was calculated as $1/\tau_{off\text{-}1}$. In contrast, the long-lived events ($\tau_{off\text{-}2}$) were voltage dependent, and attributed to major partitioning of the polypeptides into the pore lumen (Fig. 3c) (Movileanu et al. 2005).

The rate constants of dissociation $k_{off\text{-}2}$ decreased and then increased with the transmembrane potential (Fig. 3c). A simple interpretation is as follows: at transmembrane potentials lower than a threshold value V_c, the majority of transient polypeptide-induced current blockades are attributed to binding and release backward to the *trans* side. In contrast, at transmembrane potentials greater than V_c, the majority of the transient current blockades are attributed to binding and release forward to the *cis* side. One immediate issue is the discrimination between the release of the polypeptide forward to the *cis* side and the release of the polypeptide backward to the aqueous phase from which it came from. In principle, a single transient polypeptide-induced current blockade cannot be a diagnostic for the "true" translocation of the polypeptide from one side of the lipid bilayer to the other. Nevertheless, with careful calculations and voltage-dependent single-channel experiments, one can determine the fraction of single-channel events attributed to the "true" translocation for a given value of the transmembrane potential (Movileanu et al. 2005).

At a transmembrane potential of +80 mV, single-channel electrical recordings carried out with the WT-αHL protein pore in the presence of 34 μM Cox IV polypeptide revealed transient current blockades with the association rate constants: $k_{on\text{-}1} = (0.20 \pm 0.02) \times 10^5\ M^{-1}\ s^{-1}$ and $k_{on\text{-}2} = (0.60 \pm 0.03) \times 10^5\ M^{-1}s^{-1}$ (n = 3 experiments). The dissociation rate constants were $k_{off\text{-}1} = (0.76 \pm 0.01) \times 10^3\ s^{-1}$ and $k_{off\text{-}2} = (0.11 \pm 0.01) \times 10^3\ s^{-1}$, respectively ($n = 3$, Fig. 2a). When the K131D$_7$ pore was employed, the Cox IV polypeptide produced transient current blockades with the association rate constants $k_{on\text{-}1} = (0.30 \pm 0.11) \times 10^5\ M^{-1}\ s^{-1}$ and $k_{on\text{-}2} = (0.90 \pm 0.15) \times 10^5\ M^{-1}\ s^{-1}$, and the dissociation rate constants $k_{off\text{-}1} = (2.1 \pm 1.3) \times 10^3\ s^{-1}$ and $k_{off\text{-}2} = (0.16 \pm 0.04) \times 10^3\ s^{-1}$, respectively (Fig. 2b). In contrast to WT-αHL and K131D$_7$, the short-lived events were not observed with K147D$_7$ ($k_{on\text{-}2} = (0.80 \pm 0.03) \times 10^5\ M^{-1}\ s^{-1}$, $k_{off\text{-}2} = (4.8 \pm 0.6) \times 10^3\ s^{-1}$, $n = 3$) and K131D$_7$/K147D$_7$ ($k_{on\text{-}2} = 5.0 \pm 0.1) \times 10^5\ M^{-1}\ s^{-1}$, $k_{off\text{-}2} = (2.2 \pm 0.2) \times 10^3\ s^{-1}$ ($n = 3$, Fig. 2c, d), as tested by a LLR protocol (Movileanu et al. 2003, 2005). Although these long-lived

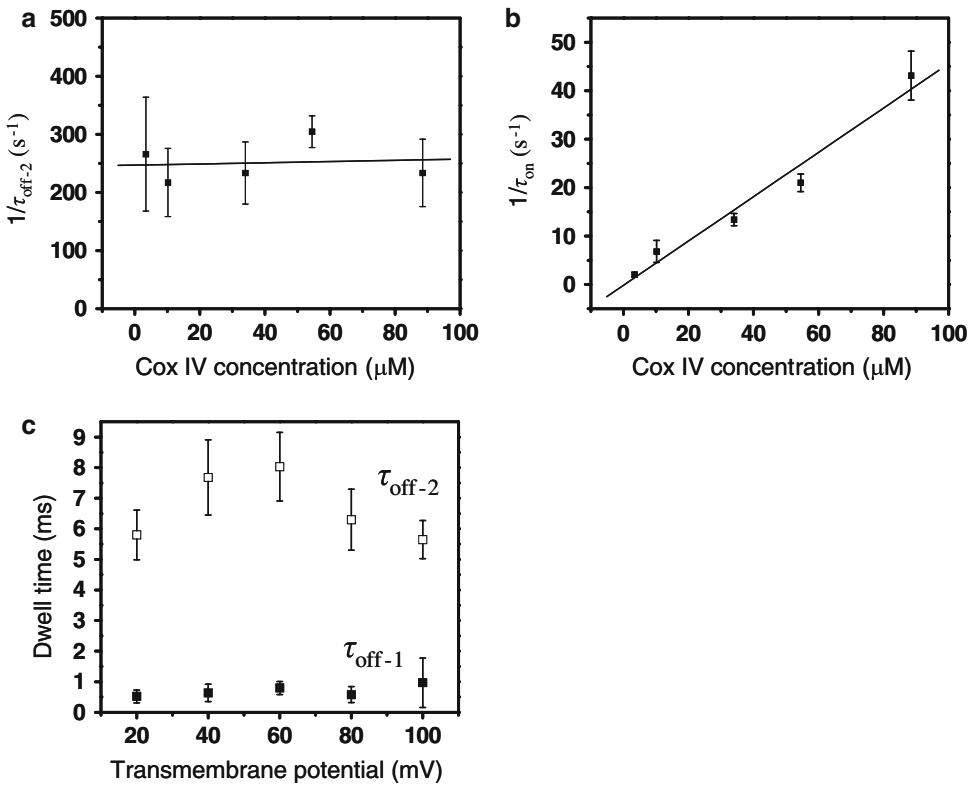

Fig. 3 The kinetics of the polypeptide–pore interaction has a bimolecular nature. The figure illustrates an example of the data recorded with the single trap-containing K147D$_7$ pore interacting with the Cox IV polypeptide: **a** The dose-response dependence of the $1/\tau_{off\text{-}2}$ values, **b** The dose-response dependence of the $1/\tau_{on}$ values, **c** The voltage-dependence of the rate constants of dissociation $\tau_{off\text{-}1}$ and $\tau_{off\text{-}2}$. The concentration of the polypeptide was 34 μM. All measurements were carried out at room temperature in 1 M KCl, 10 mM potassium phosphate, pH 7.4. The transmembrane potential was +80 mV

events were much shorter than those observed with the WT-αHL and K131D$_7$ pores, they underwent the same biphasic voltage dependence as mentioned above.

The rate constants of association (k_{on}) and dissociation ($k_{off\text{-}2}$) were dependent not only on the features of the electrostatic trap-containing αHL pore, but also the nature of the interacting cationic polypeptide. The rate constant k_{on} spanned several orders of magnitude. In Fig. 4, we show the total event frequency, which is proportional to k_{on} (see "Materials and methods"), recorded at a transmembrane potential of +80 mV. The rate constant of association k_{on} was substantially lower for more hydrophobic polypeptides (AK and AK$_D$) than for less hydrophobic (Cox IV) and hydrophilic (Syn B2) polypeptides. Therefore, the free-energy barrier for the polypeptides to pass the pore was greater for hydrophobic polypeptides, most likely due to the hydrophilic nature of the pore interior. On the other hand, the rate constant of dissociation ($k_{off\text{-}2}$) observed with the unfolded AK$_{DL}$ polypeptide was greater than that value probed with the α-helical AK polypeptide. For example, for the WT-αHL pore, we observed the values of the rate constants of dissociation $k_{off\text{-}2}$ of $\sim 3.7 \times 10^3$ and $\sim 1.3 \times 10^3$ s^{-1} with the AK$_{DL}$ and AK polypeptides, respectively. Since the only difference between these polypeptides is the folding state, this result is in excellent agreement with previous work in this laboratory, which suggested that folded polypeptides spend a longer transit time than unstructured or misfolded ones (Goodrich et al. 2007).

The position of the binding site qualitatively altered the flux of cationic polypeptides through the αHL pore. The total event frequency recorded with the K131D$_7$ pore was much higher than that recorded with the WT-αHL pore. This result is conceivable, given the location of the electrostatic trap near aqueous phase. The strong electrostatic interactions between the positively charged polypeptide and the negatively charged K131D trap is expected to dramatically alter the free-energy landscape of the polypeptide-pore interaction (see below). In contrast, the event frequency underwent moderate change when the K147D$_7$ pore was employed. Intuitively, this finding seems to be correct, given the position of the electrostatic trap, which is ~45 Å away from the aqueous phase. Therefore, the free-energy barrier for the polypeptide to cross the entry of the αHL pore was not substantially changed by the presence of the K147D trap.

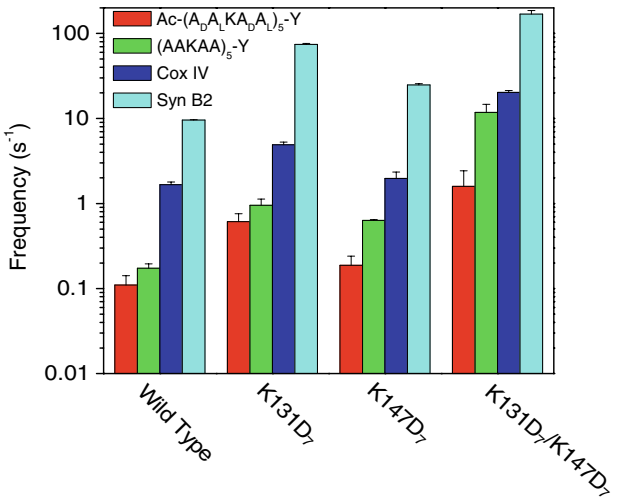

Fig. 4 The total event frequency determined from single-channel recordings with wild type and engineered αHL pores in the presence of 34 μM polypeptide added to the *trans* side of the bilayer. The other conditions are the same as those mentioned in Fig. 2. The values represent means ± SD's calculated from three separate single-channel experiments

Remarkably, the single-channel data obtained with the double trap-containing αHL pore revealed a substantial increase in the total event frequencies (Fig. 4). This result suggests that at least a second mechanism, in addition to the alteration of the entry barrier, is responsible for the dramatic change of the total event frequency recorded with the double trap-containing K131D$_7$/K147D$_7$ pore. Another interesting result was that the dissociation rate constants $k_{off\text{-}2}$ recorded with the single K147D trap-containing αHL pore significantly increased by comparison with the K147D trap-lacking αHL pores. For example, for the Syn B2 polypeptide, the rate constant of dissociation $k_{off\text{-}2}$ observed with the WT-αHL, K131D$_7$, K147D$_7$ and K131D$_7$/K147D$_7$ pores was $(0.37 \pm 0.02) \times 10^3$, $(0.33 \pm 0.04) \times 10^3$, $(7.2 \pm 1.2) \times 10^3$ and $(11 \pm 1) \times 10^3$ s^{-1}, respectively. A qualitative interpretation of these results is provided below.

A simple kinetic model of the polypeptide-pore interaction with multiple electrostatic traps

In the second part of this paper, we present a simplified model of the free-energy landscape of the polypeptide-pore interaction. The kinetic data obtained from single-channel electrical recordings with various engineered αHL protein pores and cationic polypeptides (Fig. 1b) can simply be rationalized in terms of a 1-D motion along a reaction coordinate x with a free-energy $G(x)$. Previous work examining the interaction of alanine-based polypeptides with the WT-αHL pore unraveled the presence of a binding site within the pore lumen due to the constriction of the β-barrel part of the pore (Movileanu et al. 2005). The free-energy landscape for the polypeptide-pore interaction can be represented as a two-barrier, and single-well profile (Fig. 5a).

At zero transmembrane potential, the rate constants to exit the αHL pore are shown the following scheme:

$$T \xleftarrow{k_-} P \xrightarrow{k_+} C \qquad (1)$$

where T and C stand for the *trans* and *cis* sides of the lipid bilayer, respectively. P is the binding site within the pore

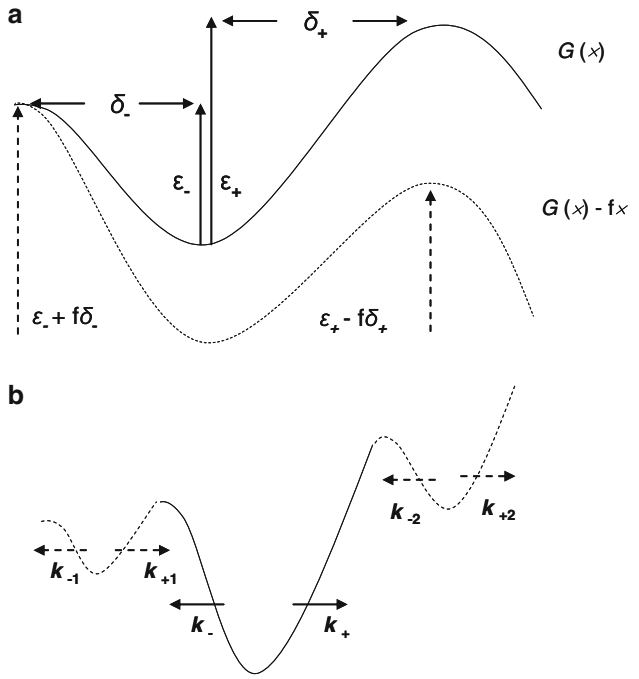

Fig. 5 The free-energy landscape of the polypeptide–pore interaction: **a** The WT-αHL pore, **b** the double trap-containing $K131D_7$/$K147D_7$ pore. In the **a**, the *continuous line* represents the free-energy landscape at zero transmembrane potential. The *dotted line* indicates the hypothetical free-energy landscape at transmembrane potentials greater than zero

lumen (Movileanu et al. 2005). Here, k_- and k_+ is the voltage-independent rate constant for the backward and forward reaction, respectively:

$$k_-(0) = \gamma e^{-\frac{\varepsilon_-}{k_B T}} \tag{2}$$

$$k_+(0) = \gamma e^{-\frac{\varepsilon_+}{k_B T}} \tag{3}$$

where γ is the transmission coefficient (Hanggi et al. 1990). k_B and T denotes the Boltzmann's constant and the absolute temperature, respectively. Here, ε_- and ε_+ indicate the free-energy barrier for the entry and exit through the αHL protein pore, respectively.

The free-energy landscape for the polypeptide-pore interaction is shown in Fig. 5a. The continuous and dotted line represents the free-energy profile at zero and greater than zero transmembrane potentials, respectively. δ_- and δ_+ represents the electrical distances from the minimum of the potential to the transition state of the backward and forward reaction, respectively. At a transmembrane potential greater than zero, the free-energy landscape is tilted by $G(x)$-fx (Movileanu et al. 2005); hence, the rate constant for the backward and forward reaction is $k_-(0)e^{f\delta-}$ and $k_+(0)e^{f\delta+}$, respectively. Therefore, the overall reaction rate constant of the polypeptide to exit the αHL protein pore is given by the following expression (Hanggi et al. 1990):

$$k(f) = k_-(0)e^{f\delta_-} + k_+(0)e^{f\delta_+} \tag{4}$$

Our major hypothesis is that the electrostatic trap, either on the *trans* opening of the αHL pore (K131D) or on the *cis* end of the β barrel (K147D) implies an additional minimum (i.e., binding site) in the free-energy landscape. We envision that for a system containing two binding sites (i.e., two minima), there are two possibilities: (1) the minima and the transition states in the free-energy landscape are far away from each. In this case, they have an independent contribution to the overall kinetics, and (2) the minima and the transition states are near to each other, so the transition state with the higher energetic barrier reduces, resulting in a faster rate constant for the polypeptide to exit the αHL protein pore. In accord with our hypothesis, the electrostatic trap K131D produced some increase in the rate constant of association k_{on} (Fig. 4), altering the entry barrier, near the *trans* opening of the pore (Fig. 5a). In contrast, the electrostatic trap on the *cis* end of the β barrel (Fig. 1) produced a significant increase in the rate constant of dissociation $k_{off\text{-}2}$ (Fig. 2), altering the exit barrier on the *cis* end of the β barrel (Figs. 1, 5b).

For the double trap-containing $K131D_7$/$K147D_7$ pore, there are two minima that correspond to the electrostatic traps K131D and K147D, respectively, and one minimum that corresponds to the native binding site, near the pore constriction (Movileanu et al. 2005) (Fig. 5b). The K131D trap alters the rate constant of association $k_{on\text{-}2}$, and the K147D trap changes the rate constant of dissociation $k_{off\text{-}2}$. Overall, both electrostatic traps increase the rate constants $k_{on\text{-}2}$ and $k_{off\text{-}2}$ (Figs. 2, 3, 4, 5).

Interaction of a folded protein with a transmembrane protein pore

In the third part of this article, we expand the complexity of the polypeptide-pore interactions by employing a folded pb_2-Ba protein that consists of the N-terminal region of pre-cytochrome b_2 (pb_2) fused to the N-terminus of the small ribonuclease barnase (Ba) (Fig. 1c). The N-terminal pb_2 fragment of the protein pb_2-Ba is positively charged, and functions as a leading domain that facilitates a strong protein-pore interaction. The folded Ba domain lies at the C-terminus and exhibits a significant entropic penalty to enter the pore, because its diameter, which ranges between 35 and 43 Å, is much greater than the narrowest inner diameter of the β-barrel part of the αHL protein pore ($\sim$15 Å).

We employed three proteins with varying leading sequence, pb_2(35)-Ba, pb_2(65)-Ba and pb_2(95)-Ba, representing the first 35, 65, and 95 residues of the pre-cytochrome b_2, respectively, fused to the Ba domain. Although the density of the positive charge is similar for

these pb_2 presequences ($\sim$0.2 per residue length), the total charge increases with the pb_2 length, as following: 7, 13, and 16, respectively. Given the location of the K147D electrostatic trap, far away from the aqueous phase ($\sim$45 Å), we explored the interaction of the pb_2-Ba proteins with a single trap-containing $K147D_7$ pore (Fig. 1a). The tilting of the free-energy landscape (dotted curve, Fig. 5a) would suggest that the pulling force on the pb_2 presequence due to the transmembrane potential is high enough to compensate the large entropic penalty of the pb_2-Ba protein to partition into the pore lumen. The single-channel electrical recordings were accomplished at +20, +30, and +40 mV, with the protein sample added to the *trans* side of the lipid bilayer. Representative single-channel electrical traces are shown in Fig. 6.

We observed a dramatic change in the kinetics of transient protein-induced current blockades when different transmembrane potentials and pb_2 presequences were examined. The response in the single-channel electrical traces varied from infrequent and very short current blockades observed with the $pb_2(35)$-Ba protein at +20 mV ($k_{on} = (1.1 \pm 0.6) \times 10^5\ M^{-1}\ s^{-1}$, $k_{off} = (2.1 \pm 1.0) \times 10^2\ s^{-1}$, $n = 3$, Fig. 6a), to transient long-lived current blockades measured with the $pb_2(65)$-Ba protein at +30 mV ($k_{on} = (2.9 \pm 0.6) \times 10^4\ M^{-1}\ s^{-1}$, $k_{off} = (9.3 \pm 4.0) \times 10^{-3}\ s^{-1}$, $n = 3$, Fig. 6b), and permanent full current blockades recorded with the $pb_2(95)$-Ba protein at +40 mV ($n = 3$, Fig. 6c). The broad changes in the rate constants of association and dissociation indicate that an array of factors contribute to the overall protein–pore interaction, revealing both driving and electrostatic forces. Moreover, permanent current blockades recorded with all pb_2 presequences at very high transmembrane potentials suggest that the pb_2-Ba proteins partition into the pore lumen, but they are released backward to the *trans* aqueous phase. For example, Fig. 6c illustrates that the pb_2-Ba protein is arrested within the pore lumen for long periods, in the range of minutes. This result is consistent with a very high energetic barrier for the pb_2-Ba protein to traverse the αHL pore from one side of the lipid bilayer to the other.

Temperature-dependent entropic repulsion of the folded Ba domain from the protein pore

Finally, to reveal the entropic repulsion of the folded Ba domain from the protein pore, we employed single-channel recordings at room temperature and at elevated temperatures ($\sim$55°C). It is conceivable that at $\sim$55°C, the thermal fluctuations of the folded Ba domain are amplified, and the polypeptide undergoes a transition to a high-free-energy state. Therefore, the energetic barrier for partitioning into the pore lumen will be drastically reduced, enhancing the rates constants of association and dissociation. We also wanted to minimize the effect of the strong pulling forces on the pb_2 presequence due the transmembrane potential, choosing a $K131D_7$ pore instead. Therefore, we assumed that the interaction takes place near the *trans* opening of the αHL protein pore (Fig. 1c). When a single WT-αHL pore was reconstituted into a lipid bilayer, the addition of $pb_2(95)$-Ba to the *trans* side produced very short-lived and infrequent current spikes ($k_{on} = (3.0 \pm 0.5) \times 10^5\ M^{-1}\ s^{-1}$, $k_{off} = (3.2 \pm 0.6) \times 10^3\ s^{-1}$, $n = 3$, Fig. 7a). WT-αHL exhibits no current blockades at room temperature (+80 mV, data not shown). We observed no current blockades produced by $pb_2(95)$-Ba in the absence of the αHL pore (channel-free bilayer, data

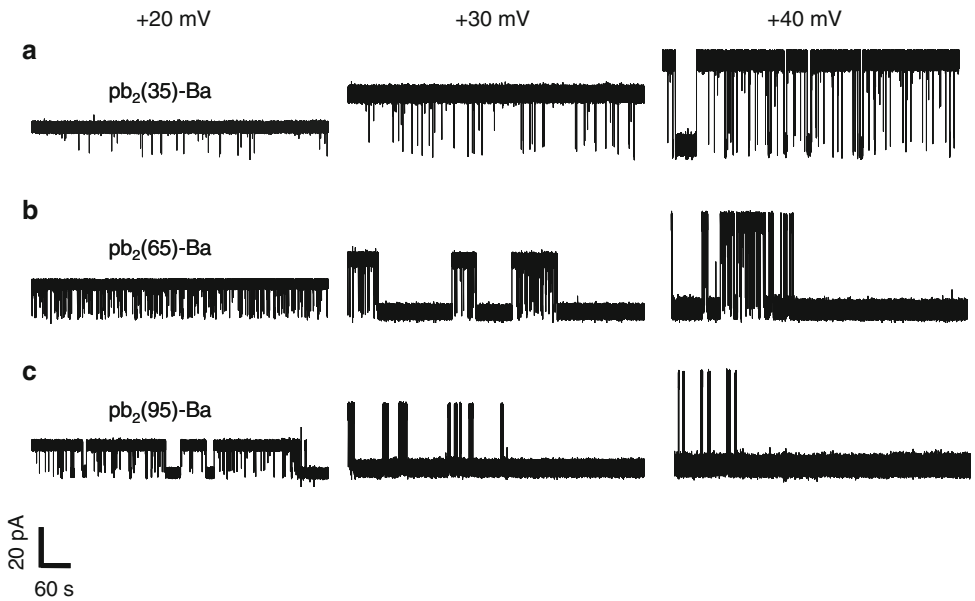

Fig. 6 Interaction of the pb_2-Ba proteins with the single trap-containing $K147D_7$ pore recorded at various transmembrane potentials. The figure illustrates representative single-channel electrical recordings for: **a** $pb_2(35)$-Ba, **b** $pb_2(65)$-Ba and **c** $pb_2(95)$-Ba. 200 nM protein was added to the *trans* side of the bilayer. The experiments were conducted at room temperature, and in 1 M KCl, 10 mM potassium buffer, pH 7.4. All single-channel electrical traces were low-pass Bessel filtered at 2 kHz

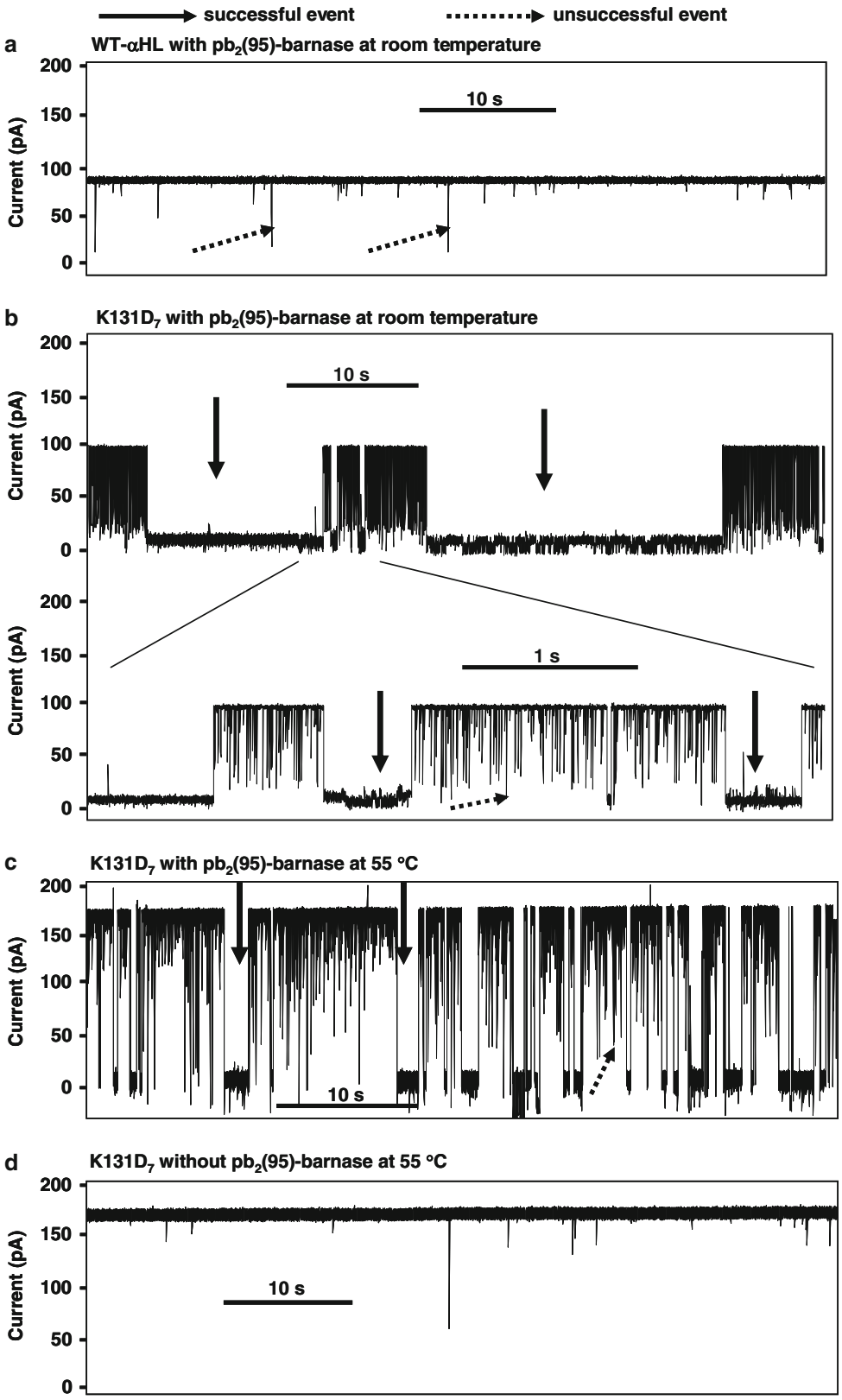

Fig. 7 Interaction of the $pb_2(95)$-Ba protein with the $K131D_7$ pore: **a** Interaction of $pb_2(95)$-Ba with a single WT-αHL protein pore at room temperature, **b** Interaction of $pb_2(95)$-Ba with a single $K131D_7$ protein at room temperature; the *upper panel* is a single-channel trace that shows two successful long-lived events; the *bottom panel* is an expansion of the trace indicated in the *upper panel*, **c** Interaction of $pb_2(95)$-Ba with a single trap-containing $K131D_7$ protein at 55°C, **d** A single-channel electrical trace of a single trap containing $K131D_7$ protein in the absence of $pb_2(95)$-Ba, and recorded at 55°C. The concentration of $pb_2(95)$-Ba, added to the *trans* side of the bilayer, was 50 nM. The transmembrane potential was +80 mV

not shown). Therefore, the spikes in Fig. 7a are ascribed to transient excursions of the pb_2-Ba protein into the WT-αHL pore.

When the WT-αHL pore was replaced by the single trap-containing $K131D_7$ pore, we observed transient long-lived ($k_{on} \sim 8.0 \times 10^5\ M^{-1}\ s^{-1}$, $k_{off} \sim 0.1\ s^{-1}$, also

called "successful"), and short-lived protein-induced current blockades (k_{on} = (1.0 ± 0.2) × 10^9 M^{-1} s^{-1}, k_{off} = (3.5 ± 0.1) × 10^3 s^{-1}, n = 3, also called "unsuccessful", Fig. 7b). More than likely, a substantially increased $k_{on\text{-}1}$, which corresponds to the short-lived events recorded with the $K131D_7$ pore, is a result of the strong electrostatic interactions between the positively charged $pb_2(95)$ presequence and the electrostatic trap engineered on the *trans* opening of the pore (Fig. 1a). Furthermore, the rate constant of association and dissociation corresponding to the long-lived current blockades increased by increasing the temperature (Fig. 7c). At 55°C, their values were $k_{on\text{-}2}$ ~3.6 × 10^8 M^{-1} s^{-1} and $k_{off\text{-}2}$ ~1.1 s^{-1}. As a control experiment, we have examined a single trap-containing $K131D_7$ pore at 55°C, and found no temperature-induced current blockades (Fig. 7d), again revealing the exceptional stability of the αHL pore.

Together, these experiments demonstrate the robustness of the engineered αHL proteins for pulling small folded proteins across a β-barrel pore. The single-channel data are instructive, indicating that the positively charged $pb_2(95)$ presequence is not sufficient for the pb_2-Ba protein to undergo a substantial partition into the pore lumen (i.e., Fig. 7a). Therefore, an electrostatic trap within the pore lumen is required for the protein substrate to produce transient long-lived current blockades.

Concluding remarks

In this article, we show a single-channel study with a β-barrel protein that interacts strongly with positively charged model and presequence polypeptides and small folded proteins. The kinetics of the polypeptide-pore interaction is dependent on the location of the trap. Such a single-molecule experiment opens many exciting opportunities for exploring the mechanisms by which the proteins interact with receptors or protein translocases. While further experimentation combined with structural analysis and computation is required, it is clear from this study that the prognosis is excellent for the interaction of small folded proteins with a transmembrane β-barrel pore.

In this work, we were not able to obtain a complete translocation of the pb_2-Ba proteins from one side of the lipid bilayer to the other. It is likely that the following two fundamental reasons caused this finding: a large entropic barrier of the folded Ba domain to move from the aqueous phase to the narrowest β-barrel domain of the αHL protein pore, and the heterogeneity of the positive and negative charges along the polypeptide chain, which is in contrast to the heavily and uniformly charged nucleic acids (Kasianowicz et al. 1996). The αHL pores are quite robust and tractable proteins, indicating that single-channel recordings can be accomplished under harsh experimental conditions in the future. This might allow the examination of the translocation of less-folded proteins in the presence of chemical denaturants, such as guanidinium hydrochloride (Oukhaled et al. 2007) and urea (Pastoriza-Gallego et al. 2007). Indeed, recent studies in Loic Auvray's group indicated that the wild-type αHL protein pore exhibits an extraordinary stability in the presence of urea, with concentrations ranging up to 7.2 M (Pastoriza-Gallego et al. 2007).

This work will nicely complement recent efforts in the molecular dynamics (MD) simulations area that establish the fundamental methodologies for examining the transport of polypeptides through protein channels (Kirmizialtin et al. 2004, 2006; Huang et al. 2005; Tian and Andricioaei 2005; Contreras Martinez et al. 2006; West et al. 2006; Goodrich et al. 2007; Makarov 2007; Wells et al. 2007). On the other hand, this work does not address the long list of outstanding questions that surround the molecular mechanisms of the protein translocases and receptors; (a) How do various N-terminal presequences recognize the membrane by receptors? (b) How do the folding features of the protein domains alter the translocation kinetics? (c) How do various hydrophobic and hydrophilic parts of the protein substrate interact with the β-barrel wall? Recent advances in single-molecule technology and protein engineering show the promise, identifying the complexity of the translocation machineries and providing more realistic models for the protein traffic across biological membranes (Koriazova and Montal 2003; Melnyk and Collier 2006; Fischer and Montal 2007).

Acknowledgments The authors thank Andreas Matouschek for providing the pb_2-Ba proteins, Steve Cheley for supplying the αHL-RL3 plasmids, Aaron J. Wolfe for his help during the preliminary stage of this work, and Hagan Bayley, Dmitrii Makarov, and Serdal Kirmizialtin for stimulating discussions. This work was supported by Syracuse University start-up funds, and the US National Science Foundation DMR-706517 (to L.M.).

References

Becker L, Bannwarth M, Meisinger C, Hill K, Model K, Krimmer T, Casadio R, Truscott KN, Schulz GE, Pfanner N, Wagner R (2005) Preprotein translocase of the outer mitochondrial membrane: reconstituted Tom40 forms a characteristic TOM pore. J Mol Biol 353:1011–1020

Cheley S, Braha G, Lu XF, Conlan S, Bayley H (1999) A functional protein pore with a "retro" transmembrane domain. Protein Sci 8:1257–1267

Chen YX, Mant CT, Hodges RS (2003) Temperature selectivity effects in reversed-phase liquid chromatography due to conformation differences between helical and non-helical peptides. J Chromatogr A 1010:45–61

Contreras Martinez LM, Martinez-Veracoechea FJ, Pohkarel P, Stroock AD, Escobedo FA, DeLisa MP (2006) Protein

translocation through a tunnel induces changes in folding kinetics: a lattice model study. Biotechnol Bioeng 94:105–117
Delano WL (2007) DeLano Scientific. San Carlos, CA
Fischer A, Montal M (2007) Single molecule detection of intermediates during botulinum neurotoxin translocation across membranes. Proc Natl Acad Sci USA 104:10447–10452
Gabriel K, Buchanan SK, Lithgow T (2001) The alpha and the beta: protein translocation across mitochondrial and plastid outer membranes. Trends Biochem Sci 26:36–40
Goodrich CP, Kirmizialtin S, Huyghues-Despointes BM, Zhu AP, Scholtz J.M., Makarov DE, Movileanu L (2007) Single-molecule electrophoresis of beta-hairpin peptides by electrical recordings and Langevin dynamics simulations. J Phys Chem B 111:3332–3335
Guiard B (1985) Structure, expression and regulation of a nuclear gene encoding a mitochondrial protein: the yeast L(+)-lactate cytochrome c oxidoreductase (cytochrome b2). EMBO J 4:3265–3272
Halverson KM, Panchal RG, Nguyen TL, Gussio R, Little SF, Misakian M, Bavari S, Kasianowicz JJ (2005) Anthrax biosensor, protective antigen ion channel asymmetric blockade. J Biol Chem 280:34056–34062
Hanggi P, Talkner P, Borkovec M (1990) Reaction-rate theory - 50 years after kramers. Rev Mod Phys 62:251–341
Hinnah SC, Wagner R, Sveshnikova N, Harrer R, Soll J (2002) The chloroplast protein import channel Toc75: Pore properties and interaction with transit peptides. Biophys J 83:899–911
Howorka S, Movileanu L, Braha O, Bayley H (2001) Kinetics of duplex formation for individual DNA strands within a single protein nanopore. Proc Natl Acad Sci USA 98:12996–13001
Huang S, Ratliff KS, Matouschek A (2002) Protein unfolding by the mitochondrial membrane potential. Nat Struct Biol 9:301–307
Huang L, Kirmizialtin S, Makarov DE (2005) Computer simulations of the translocation and unfolding of a protein pulled mechanically through a pore. J Chem Phys 123:124903
Jung Y, Bayley H, Movileanu L (2006) Temperature-responsive protein pores. J Am Chem Soc 128:15332–15340
Kang XF, Gu LQ, Cheley S, Bayley H (2005) Single protein pores containing molecular adapters at high temperatures. Angew Chem Int Ed Engl 44:1495–1499
Karginov VA, Nestorovich EM, Moayeri M, Leppla SH, Bezrukov SM (2005) Blocking anthrax lethal toxin at the protective antigen channel by using structure-inspired drug design. Proc Natl Acad Sci USA 102:15075–15080
Kasianowicz JJ, Brandin E, Branton D, Deamer DW (1996) Characterization of individual polynucleotide molecules using a membrane channel. Proc Natl Acad Sci USA 93:13770–13773
Kirmizialtin S, Ganesan V, Makarov DE (2004) Translocation of a beta-hairpin-forming peptide through a cylindrical tunnel. J Chem Phys 121:10268–10277
Kirmizialtin S, Huang L, Makarov DE (2006) Computer simulations of protein translocation. Phys Stat Sol (b) 243:2038–2047
Koriazova LK, Montal M (2003) Translocation of botulinum neurotoxin light chain protease through the heavy chain channel. Nat Struct Biol 10:13–18
Krantz BA, Melnyk RA, Zhang S, Juris SJ, Lacy DB, Wu Z, Finkelstein A, Collier RJ (2005) A phenylalanine clamp catalyzes protein translocation through the anthrax toxin pore. Science 309:777–781
Krantz BA, Finkelstein A, Collier RJ (2006) Protein translocation through the anthrax toxin transmembrane pore is driven by a proton gradient. J Mol Biol 355:968–979
Krasilnikov OV, Bezrukov SM (2004) Polymer partitioning from nonideal solutions into protein voids. Macromolecules 37:2650–2657
Krasilnikov OV, Merzlyak PG, Yuldasheva LN, Rodrigues CG, Bhakdi S, Valeva A (2000) Electrophysiological evidence for heptameric stoichiometry of ion channels formed by Staphylococcus aureus alpha-toxin in planar lipid bilayers. Mol Microbiol 37:1372–1378
Krasilnikov OV, Rodrigues CG, Bezrukov SM (2006) Single polymer molecules in a protein nanopore in the limit of a strong polymer-pore attraction. Phys Rev Lett 97:018301
Krause E, Bienert M, Schmieder P, Wenschuh H (2000) The helix-destabilizing propensity scale of D-amino acids: the influence of side chain steric effects. J Am Chem Soc 122:4865–4870
Kyte J, Doolittle RF (1982) A simple method for displaying the hydropathic character of a protein. J Mol Biol 157:105–132
Makarov DE (2007) Unraveling individual molecules by mechanical forces: theory meets experiment. Biophys J 92:4135–4136
Matouschek A, Glick BS (2001) Barreling through the outer membrane. Nat Struct Biol 8:284–286
Matouschek A, Azem A, Ratliff K, Glick BS, Schmid K, Schatz G (1997) Active unfolding of precursor proteins during mitochondrial protein import. EMBO J 16:6727–6736
Mauguen Y, Hartley RW, Dodson EJ, Dodson GG, Bricogne G, Chothia C, Jack A (1982) Molecular structure of a new family of ribonucleases. Nature 297:162–164
McManus OB, Magleby KL (1988) Kinetic states and modes of single large-conductance calcium-activated potassium channels in cultured rat skeletal-muscle. J Physiol (Lond) 402:79–120
Melnyk RA, Collier RJ (2006) A loop network within the anthrax toxin pore positions the phenylalanine clamp in an active conformation. Proc Natl Acad Sci USA 103:9802–9807
Menestrina G (1986) Ionic channels formed by Staphylococcus-Aureus Alpha-Toxin—voltage-dependent inhibition by divalent and trivalent cations. J Membr Biol 90:177–190
Misakian M, Kasianowicz JJ (2003) Electrostatic influence on ion transport through the alphaHL channel. J Membr Biol 195:137–146
Mitchell JBO, Smith J (2003) D-amino acid residues in peptides and proteins. Proteins 50:563–571
Movileanu L, Bayley H (2001) Partitioning of a polymer into a nanoscopic protein pore obeys a simple scaling law. Proc Natl Acad Sci USA 98:10137–10141
Movileanu L, Howorka S, Braha O, Bayley H (2000) Detecting protein analytes that modulate transmembrane movement of a polymer chain within a single protein pore. Nat Biotechnol 18:1091–1095
Movileanu L, Cheley S, Howorka S, Braha O, Bayley H (2001) Location of a constriction in the lumen of a transmembrane pore by targeted covalent attachment of polymer molecules. J Gen Physiol 117:239–251
Movileanu L, Cheley S, Bayley H (2003) Partitioning of individual flexible polymers into a nanoscopic protein pore. Biophys J 85:897–910
Movileanu L, Schmittschmitt JP, Scholtz JM, Bayley H (2005) Interactions of the peptides with a protein pore. Biophys J 89:1030–1045
Muro C, Grigoriev SM, Pietkiewicz D, Kinnally KW, Campo ML (2003) Comparison of the TIM and TOM channel activities of the mitochondrial protein import complexes. Biophys J 84:2981–2989
Oukhaled G, Mathe J, Biance A-L, Bacri L, Betton J-M, Lairez D, Pelta J, Auvray L (2007) Unfolding of proteins and long transient conformations detected by single nanopore recording. Phys Rev Lett 98:158101
Paddon CJ, Hartley RW (1987) Expression of Bacillus amyloliquefaciens extracellular ribonuclease (barnase) in Escherichia coli following an inactivating mutation. Gene 53:11–19
Pastoriza-Gallego M, Oukhaled G, Mathe J, Thiebot B, Betton JM, Auvray L, Pelta J (2007) Urea denaturation of alpha-hemolysin pore inserted in planar lipid bilayer detected by single nanopore

recording: loss of structural asymmetry. FEBS Lett 581:3371–3376
Roise D, Theiler F, Horvath SJ, Tomich JM, Richards JH, Allison DS, Schatz G (1988) Amphiphilicity is essential for mitochondrial presequence function. EMBO J 7:649–653
Sackmann B, Neher E (1995) Single-channel recording. Kluwer, New York
Schwartz MP, Matouschek A (1999) The dimensions of the protein import channels in the outer and inner mitochondrial membranes. Proc Natl Acad Sci USA 96:13086–13090
Simon SM, Peskin CS, Oster GF (1992) What drives the translocation of proteins. Proc Natl Acad Sci USA 89:3770–3774
Song LZ, Hobaugh MR, Shustak C, Cheley S, Bayley H, Gouaux JE (1996) Structure of staphylococcal alpha-hemolysin, a heptameric transmembrane pore. Science 274:1859–1866
Tian P, Andricioaei I (2005) Repetitive pulling catalyzes co-translocational unfolding of barnase during import through a mitochondrial pore. J Mol Biol 350:1017–1034
Wells DB, Abramkina V, Aksimentiev A (2007) Exploring transmembrane transport through alpha-hemolysin with grid-steered molecular dynamics. J Chem Phys 127:125101
West DK, Brockwell DJ, Paci E (2006) Prediction of the translocation kinetics of a protein from its mechanical properties. Biophys J 91:L51–L53
Wickner W, Schekman R (2005) Protein translocation across biological membranes. Science 310:1452–1456
Wolfe AJ, Mohammad MM, Cheley S, Bayley H, Movileanu L (2007) Catalyzing the translocation of polypeptides through attractive interactions. J Am Chem Soc 129:14034–14041
Zakharov SD, Erukova VY, Rokitskaya TI, Zhalnina MV, Sharma O, Loll PJ, Zgurskaya HI, Antonenko YN, Cramer WA (2004) Colicin occlusion of OmpF and TolC channels: outer membrane translocons for colicin import. Biophys J 87:3901–3911